INTERACTION OF AQUATED FORM OF RUTHENIUM(III) ANTICANCER COMPLEXES WITH NORMAL AND MISMATCH BASE PAIRS

6.1 Introduction

Studies on the binding mechanism of drug molecules with DNA are found to be in the focus of many scientists during past few decades.[1] Drug-DNA interaction studies have received great attention, particularly in inhibition of DNA replication in cancer cells, understanding the structural properties of DNA, mutation of genes, origin of some diseases and reaction mechanism of antitumor and antiviral drugs.[2] In view of the fact, significant amount of works have been done to design and synthesize more efficient DNA targeted drugs and also to investigate their structure – activity relationships.[3] For the past few decades, a great deal of interest have been given to develop new potential anticancer agents in order to treat various forms of cancer and some of them are found to be effective clinical drugs.[4-8] But most of the anticancer drugs are non-selective with severe toxicity. Therefore, to develop new anticancer drugs with lower toxicity and good selectivity for the target are the major challenges to the present researchers.

Gene mutations are thought to be an initial source of evolution, as they cause alteration in the sequence of nucleotides in DNA.[9] Genomes of unicellular or multicelluler organisms are composed of billions of base pairs. During the lifecycle of these organisms, conservation and precise replication of the genetic information occur within the base structures and DNA sequences. However, at the time of replication, DNA polymerase may incorporate wrong nucleotides, giving rise to the formation of mismatched base pairs in a newly synthesized DNA duplex.[10-11] DNA mismatches may also arise from hetero-duplex formation during homologous recombination,[12] from spontaneous deamination of nucleic acid bases (e.g. thymine from 5-methylcytosine),[13] endogenous mutagens (reactive oxygen or nitrogen species), environmental damaging agents (oxidizing and alkylating chemicals) and physical factors (UV or ionizing radiations).[14] DNA mismatches leads to mutagenesis, alteration of the cellular phenotype, dysfunctions and diseases.[14] Generally, post replicative DNA repair system corrects this types of error and preserves genome integrity from endogenous and exogenous damage in all living organisms.[15-17]

However, failure of this repair may lead to xeroderma pigmentosum, hereditary nonpolyposis colon cancer, and some forms of breast cancer.[18] DNA has been reported to be a primary intracellular target for ruthenium(III) as well as other antitumor metal complexes. The drug - DNA adduct can cause DNA damage by blocking the cell division followed by death of cancer cells.[19-22] The antitumor action of ruthenium(III) complexes are the consequence of direct DNA binding and damage.[23] Novakova *et. al*. reported that the ruthenium complex *mer*-[Ru(III)(terpy)Cl_3], is able to bind DNA duplex firmly which unwinds the DNA and coordinates preferentially to isolated guanine bases.[24] Extensive DNA damage correlates with a high cytotoxicity. Clarke *et. al*. showed that a significant amount of ruthenium ions interacts with DNA after 24 hour incubation of human cervical cancer cells (HeLa) with a antitumor ruthenium(III) complex imidazolium[*trans*-$RuCl_4$(3H-imidazole)$_2$](ICR).[23] Experiment carried out by Barca *et. al*. showed that a number of ruthenium(III) complexes, including NAMI are able to bind DNA but exhibit lower interstrand cross-linking as compared to cisplatin.[25] Messori *et. al*. have demonstrated that NAMI and RAP (dichloro (1,2-propylendiaminetetraacetate) ruthenium(III) are capable of altering DNA conformation and inhibit the recognition and cleavage of DNA.[26]

We have investigated the interaction of monoaqua complexes of NAMI-A [*trans*-$RuCl_3(H_2O)$(3H-imidazole)(dmso-S)] (**Ia)** and NAMI-A type of complex [*trans*-$RuCl_3(H_2O)$(4-amino-1,2,4-triazole)(dmso-S)] (**IVa)** with normal and mismatch DNA base pairs to understand the nature of DNA damage. The aqua derivatives of ruthenium complexes are much more reactive towards DNA target than their parent chloro complexes.[27] Hence, in this study we have selected aqua derivates of ruthenium complexes. We have employed quantum chemical tools to investigate the interaction of normal base pairs (**AT** and **GC**) as well as mismatch base pairs (**AA**, **GG**, **CC**, **TT**) with ruthenium complexes **Ia** and **IVa**. Change of molecular geometry, stability, energy and electrostatic potential of ruthenium complexes due to interaction with isolated normal (**GC** and **AT**) and mismatch (**AA**, **CC**, **GG** and **TT**) base pairs have been investigated.

6.2 Computation details

GAUSSIAN 09 program package[28] is employed to carry out DFT calculation on normal (**AT** and **GC**), mismatch (**AA**, **GG**, **CC** and **TT**) base pairs and two interacting ruthenium(III) complexes using M062X functional.[29] LANL2DZ basis set[30] which describe effective core potential of Wadt and Hay (Los Alamos ECP) on ruthenium atom and 6-31+G(d,p) basis set[31] for all the nonmetal atoms are used for ground state geometry optimization. The reason for using LANL2DZ basis set is that it reduces the calculation time containing larger nuclei. The gas phase geometries of the ruthenium(III) complexes have been fully optimized using unrestricted M062X method without imposing any symmetry constrain with tight convergence criteria. Vibrational analysis has been performed at the same level of theory for achieving energy minimum. Natural bond orbital (NBO) calculations are carried out using NBO code included in Gaussian 09 program at the same level of theory.[32] Interaction energies (ΔE) of all the adducts are evaluated after the correction of the basis set superposition error.[33,34] Interaction energy (ΔE) is determined from the following equation:

$$\Delta E = E_{rutheniumcomplex-basepair} - E_{basepair} - E_{rutheniumcomplex}$$

$E_{rutheniumcomplex-basepair}$ is the energy of the optimized base pair-ruthenium adduct, $E_{basepair}$ is the energy of the optimized base pair and $E_{rutheniumcomplex}$ is the energy of optimized ruthenium complex.

6.3 Results and Discussion

6.3.1 Structural analysis

The gas phase optimized geometries of ruthenium complexes (**Ia** and **IVa)**, two isolated regular (**AT**, **GC**) and four mismatch (**AA**, **GG**, **TT** and **CC**) base pairs along with their H-bonding distances evaluated by DFT at M062X level are shown in Fig. 6.1 and Fig. 6.2. Significant geometrical parameters of the ruthenium complexes (**Ia** and **IVa)** evaluated at M062X / (LANL2DZ+6-31G(d,p)) are listed in Table 6.1. In both the ruthenium complexes, Ru^{3+} is found to be hexa-coordinated involving sulphur atom of DMSO group, nitrogen atom of imidazole, three chloride ligands and an oxygen atom of water. Ru—Cl1, Ru—Cl2 and Ru—Cl3 bond lengths of complexes **Ia** and **IVa** are in the range of 2.33-2.42 Å, while Ru—O bond length is

found to be 2.19 Å (complex **Ia**) and 2.20 Å (complex **IVa**). The Ru—N1 and Ru—S1 bond distances of complex **Ia** are calculated to be 2.09 Å and 2.36 Å, while and 2.10 Å and 2.35 Å for complex **IVa**. Bond angles Cl1—Ru—O, O—Ru—Cl2, Cl2—Ru—Cl3 and Cl3—Ru—Cl1 are in the range of 85.9-97.4^0, 81.2-84.7^0, 95.4-97.4^0, 97.4-96.8^0, respectively, for both the complexes, suggesting slightly distorted octahedral geometry around the ruthenium(III) ion. Again the dihedral angle Cl1—O—Cl2—Cl3 of complexes **Ia** and **IVa** computed using DFT are found to be 3.28^0 and 2.01^0, reflecting a marginal deviation from planarity. Hence, the observed bond angles and dihedral angles suggest the distorted octahedral structure of the ruthenium complexes. Geometrical parameters calculated at M062X level is comparable with available experimental data of NAMI.[35] However, slightly higher values of the geometrical parameters obtained by using computational methods are due to the systematic errors of computational method, basis set and environment factors.[36] The optimized geometries of all the isolated regular and mismatch base pairs are almost planar and the hydrogen bonding distances are found to be in the range 1.77 Å -1.98 Å. The structural deformations of all the optimized base pairs are found to be less than 1% in comparison with the available literatures.[37,38]

Table 6.1 Selected bond lengths (Å) and bond angles (^{0}) calculated for complex **Ia** and complex **IVa** at M062X / (LANL2DZ+6-31G(d,p)) level in the gas phase.

Parameters	Complex **Ia**	Complex **IVa**	NAMI (X-ray)
Ru—Cl1	2.38	2.39	2.345
Ru—Cl2	2.42	2.40	2.323
Ru—Cl3	2.34	2.33	2.359
Ru—Cl4			2.340
Ru—O(wat1)	2.19	2.20	
Ru—N1	2.09	2.10	2.081
Ru—S1	2.36	2.35	2.296
N1—Ru—S1	177.3	177.1	176.9
Cl1—Ru—O(wat1)	85.9	97.4	
O(wat1)—Ru—Cl2	81.2	84.7	
Cl2—Ru—Cl3	95.4	97.4	89.3
Cl3—Ru—Cl1	97.4	96.8	89.7
Cl1—Ru—Cl4			90.2
Cl1—O—Cl2—Cl3	3.28	2.01	

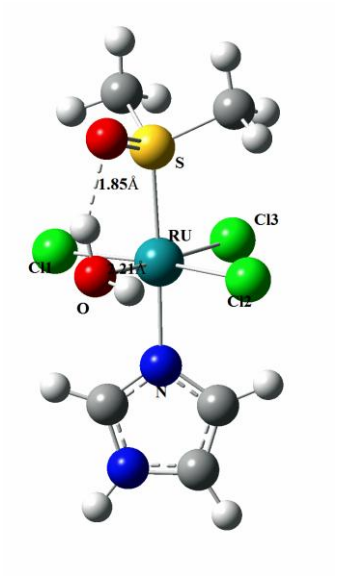

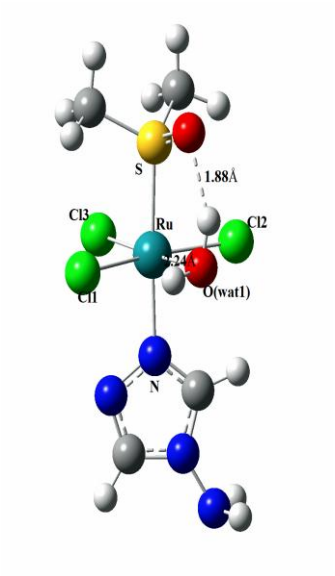

Ia **IVa**

Fig. 6.1 Optimized geometries of complex **Ia** and complex **IVa** with appropriate numbering obtained from M062X / (LanL2DZ+6-31G(d,p)) calculation.

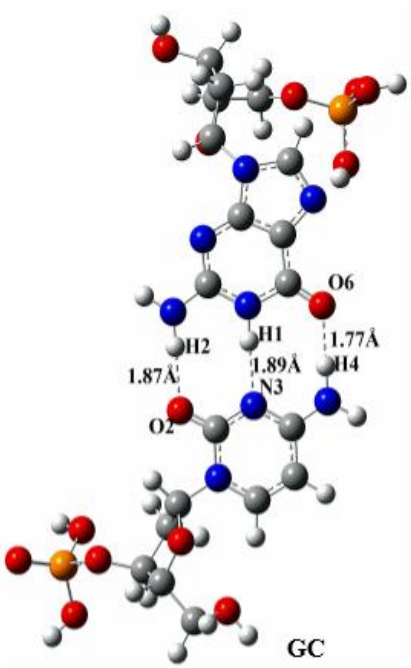

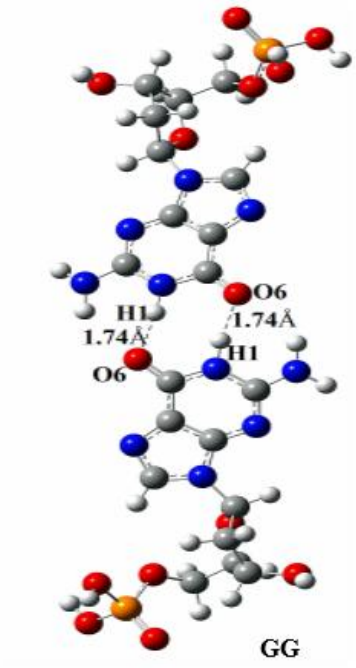

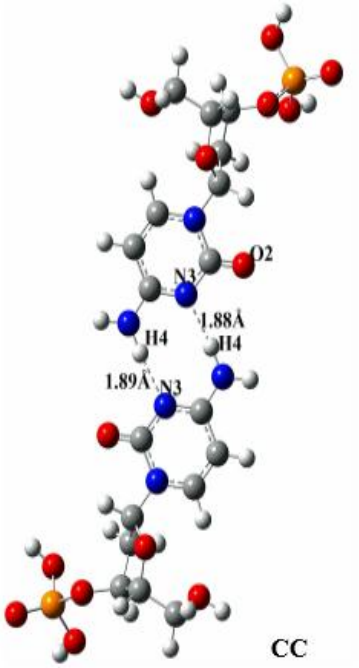

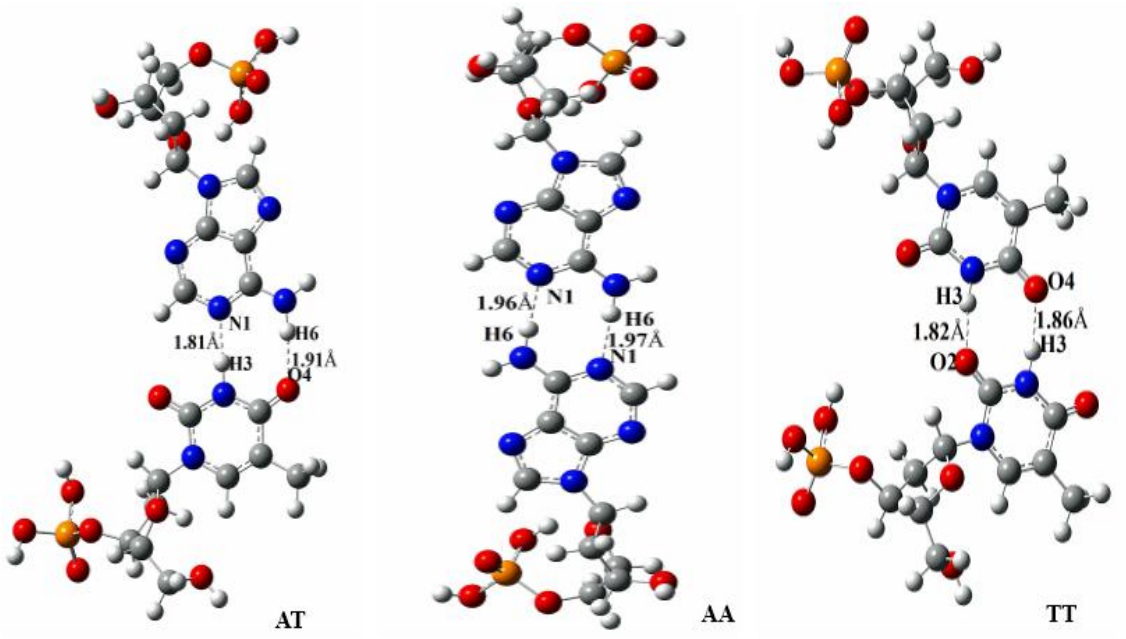

Fig. 6.2 Optimized geometries of normal and mismatch base pair with appropriate numbering obtained from M062X/ (LanL2DZ+6-31G(d,p)) calculation.

6.3.2 Structural characteristics of ruthenium complexes-base pair adduct

Significant structural parameters and optimized geometries of ruthenium complex-base pair adducts calculated at M062X / (LANL2DZ+6-31G(d,p)) level are shown in Table 6. 2 and Fig. 6.3 and Fig. 6.4. It is noticed from Table 6.2 that ruthenium atom is coordinated with N7 atom of adenine in the adducts **AT-Ia**, **AT-IVa**, **AA-Ia** and **AA-IVa** at a distance in the range of 2.13-2.19Å, while Ru—N7 bond lengths in **GC-Ia, GC-IVa, GG-Ia** and **GG-IVa** adducts are calculated to be in the range of 2.12-2.15 Å, respectively. The dihedral angle Cl1—Ru—N7— C5 in **AT-Ia**, **AA-Ia**, **AT-IVa**, **AA-IVa** adducts are found to be -53.3^0, 61.8^0 -27.4^0, -45.6^0 whereas Cl1—Ru—N7— C5 in angles **GC-Ia**, **GG-Ia**, **GC-IVa**, **GG-IVa** adducts are evaluated to be 55.9^0, -38.3, 60.0^0 and -38.6^0 respectively. Again, N7—Ru—Cl1 bond angle in all the adducts are found to be in the range of 85.8—90.9^0. The bond angle N7—Ru—Cl1 and dihedral angle Cl1—Ru—N7—C5 reveal the hexacoordinated distorted octahedral geometry of all the adducts. However, higher distortion in the geometry is observed for **CC-Ia**, **CC-IVa**, **TT-Ia** and **TT-IVa** adducts. *i.e*, geometry of the normal as well as mismatch base pairs is distorted significantly on interaction with the ruthenium complex.

Table 6.2 Calculated bond lengths (Å) and bond angles (^{0}) of ruthenium complex-base pair adduct at M062X / (LANL2DZ+6-31G(d,p)) level in the gas phase.

Parameters	Complex **Ia**						Complex **IVa**					
	GC-Ia	**GG-Ia**	**CC-Ia**	**AT-Ia**	**AA-Ia**	**TT-Ia**	**GC-IVa**	**GG-IVa**	**CC-IVa**	**AT-IVa**	**AA-IVa**	**TT-IVa**
Ru—N7	2.12	2.15		2.15	2.16		2.13	2.13		2.19	2.13	
Ru—O2			2.08						2.14			
Ru—O4						2.16						2.11
Ru—Cl1	2.35	2.39	2.46	2.41	2.43	2.38	2.34	2.45	2.48	2.36	2.42	2.39
Ru—Cl2	2.49	2.41	2.39	2.42	2.40	2.41	2.50	2.37	2.34	2.46	2.41	2.41
Ru—Cl3	2.38	2.38	2.38	2.39	2.38	2.36	2.39	2.39	2.37	2.39	2.41	2.38
Ru—S	2.40	2.42	2.43	2.44	2.39	2.40	2.40	2.43	2.46	2.43	2.44	2.40
Ru—N	2.11	2.05	2.08	2.08	2.11	2.08	2.10	2.05	2.08	2.11	2.09	2.09
Cl1—Ru—N7	89.7	86.8		87.6	89.2		90.1	87.2		88.0	88.9	
N7—Ru—Cl2	85.8	86.0		89.4	88.1		87.7	87.9		89.7	90.9	
Cl1—Ru—O2			87.7						85.8			
O2—Ru—Cl2			90.1						89.8			
Cl1—Ru—O4						85.6						85.8
O4—Ru—Cl2						85.9						90.6
Cl1—Ru—O6												
O6—Ru—Cl2												
Cl1—Ru—N7—C5	55.9	-38.3		-53.3	61.8							
Cl1—Ru—O6—H2							60.0	-38.6		-27.4	-45.6	
Cl1—Ru—O2—C2			113.0						-161.1			
Cl2—Ru—O4—C4						-33.0						-62.3

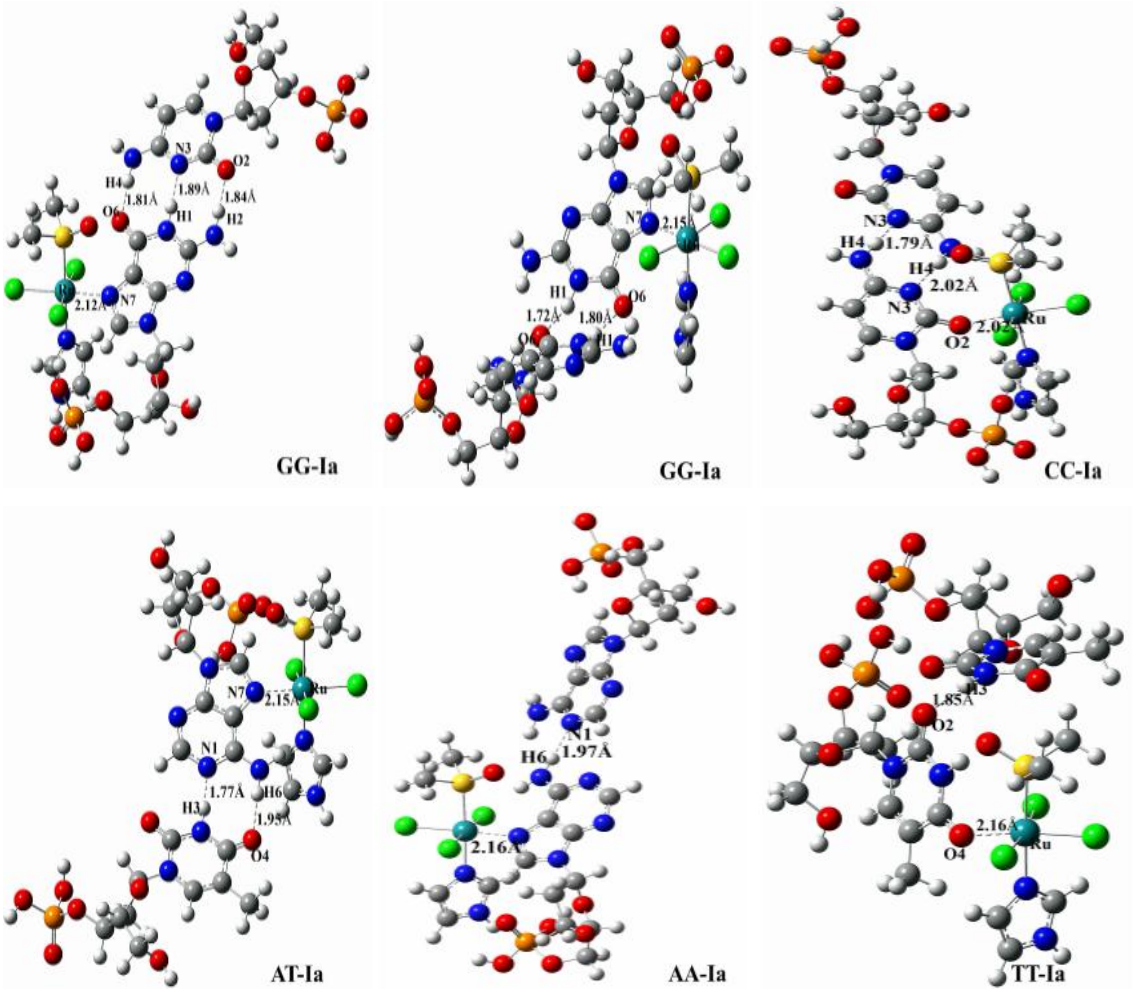

Fig. 6.3 Optimized structures of interactions of complex **Ia** with normal and mismatch base pair obtained from M062X / (LanL2DZ+6-31G(d,p)) calculation.

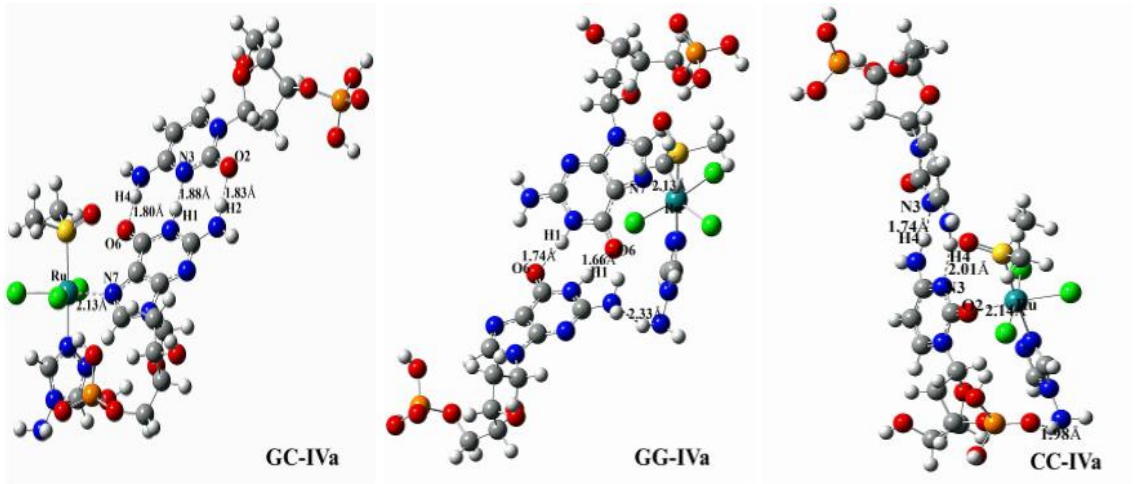

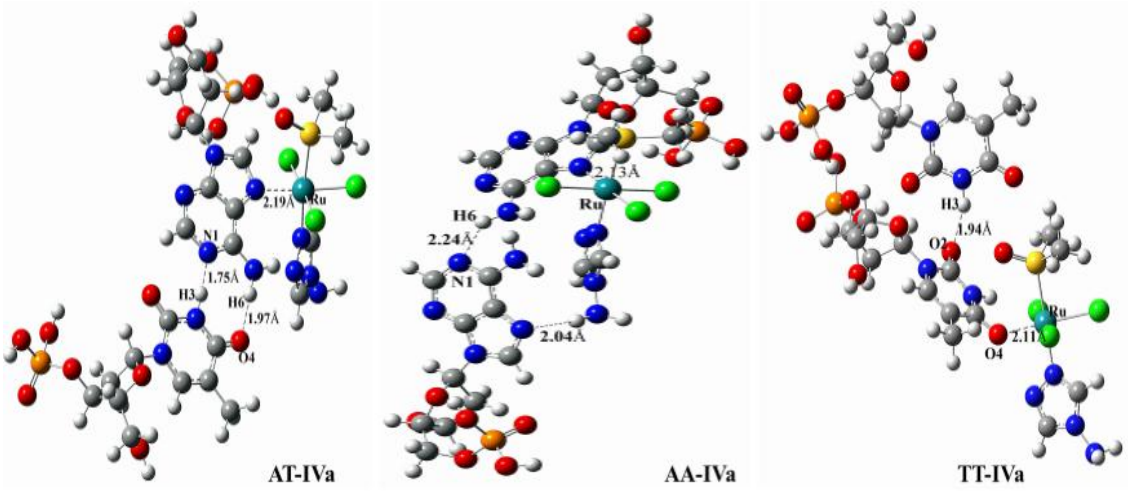

Fig. 6.4 Optimized structures of interactions of complex **IVa** with normal and mismatch base pair obtained from M062X / (LanL2DZ+6-31G(d,p)) calculation.

Table 6.3 reports the hydrogen bonding distances of base pairs in the isolated as well as complex-base pair adducts. Table 6.3 reveals that in **GC-Ia** and **GC-IVa** adducts, H2···O2 hydrogen bond distances are shorten and O6···H4 distances are found to be significantly lengthened as compared to the isolated GC base pair, while, H1···N3 distance remains almost unchanged in **GC-Ia** as well as in **GC-IVa** adducts. In **AT–Ia** adduct the H6···O4 distance increases by about 0.04Å while N1···H1 hydrogen bond separation decrease by 0.04Å, in comparison with the isolated **AT** pair. Calculated distances H6···O4 and N1···H1 in **AT–IVa** adduct are found to be 1.97 Å and 1.75 Å, respectively. In the mismatch base pairs, there are substantial lengthening in hydrogen bond distances O6···H1 of **GG-Ia**, N3···H4 of **CC**, N1···H6 of **AA** and O2···H3 of **TT** adducts while, O6···H1 distance in **GG-IVa** adduct decreases by 0.18 Å when compared with the isolated base pairs.

6.3.3 Interaction in ruthenium complex –base pair adduct

During the formation of ruthenium complex-DNA adduct, lowest unoccupied molecular orbital (LUMO) of ruthenium complex plays a significant role by accepting electrons from highest molecular orbital (HOMO) of DNA base pair.[39] The 3D isosurface plots of HOMO of DNA base pairs and LUMO of ruthenium complexes are shown in Fig. 6.5 and 6.6. It is seen from Fig. 6.5 that the electron density of HOMO is localized mainly on N7 atom of **GC**, **GG**, **AT** and **AA** base pairs and on O2 and O4 atoms of **CC** and **TT** base pairs. The electron density of LUMO in

complex **Ia** and **IVa** is mainly localized on the ruthenium atom (Fig. 6.6). Distribution of electron densities indicate that N7 atom of guanine and adenine, O2 atom cytosine, O4 atom of thymine can act as an electron donor which can readily coordinate with acceptor ruthenium atom (Fig. 6.7).

Table 6.3 Hydrogen bond distances of isolated base pair and base pair adducts calculated at M062X / (LANL2DZ+6-31G(d,p)) level of theory.

Adducts		**Ia**	**Iva**	Isolated base pair
		Hydrogen bond	Hydrogen bond	Hydrogen bond
GC	O6···H4	1.81	1.80	1.77
	H1···N3	1.90	1.88	1.90
	H2···O2	1.84	1.83	1.87
GG	O6···H1	1.80	1.66	1.74
	H1···O6	1.72	1.74	1.74
CC	N3···H4	2.02	2.01	1.89
	H4···N3	1.79	1.74	1.88
AT	H6···O4	1.95	1.97	1.91
	N1···H1	1.77	1.75	1.81
AA	N1···H6	1.97	2.24	1.96
TT	O2···H3	1.85	1.94	1.82

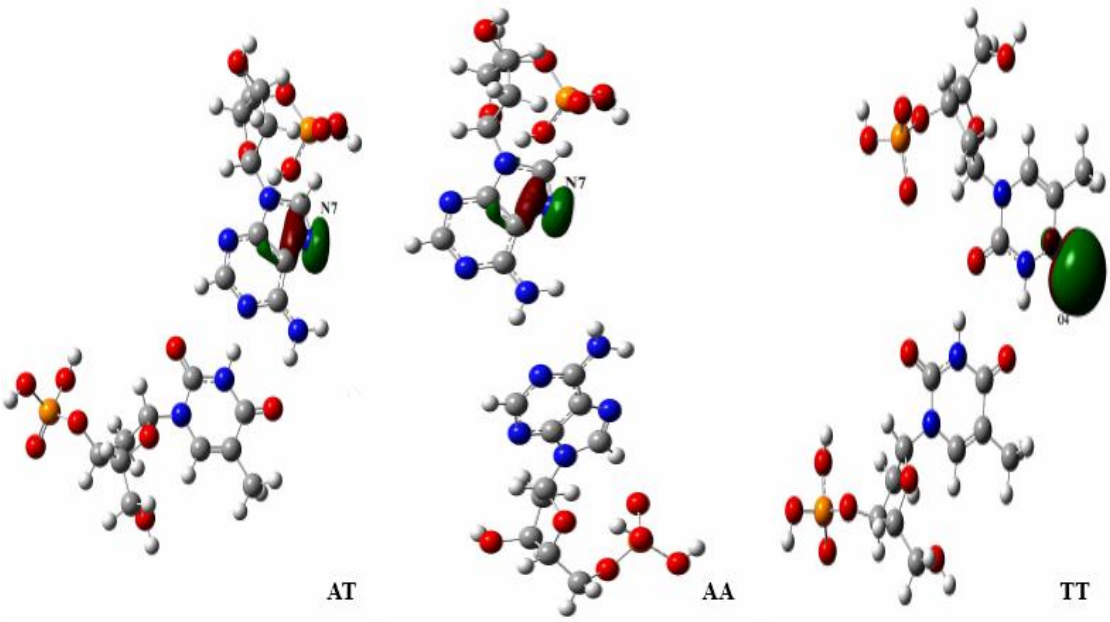

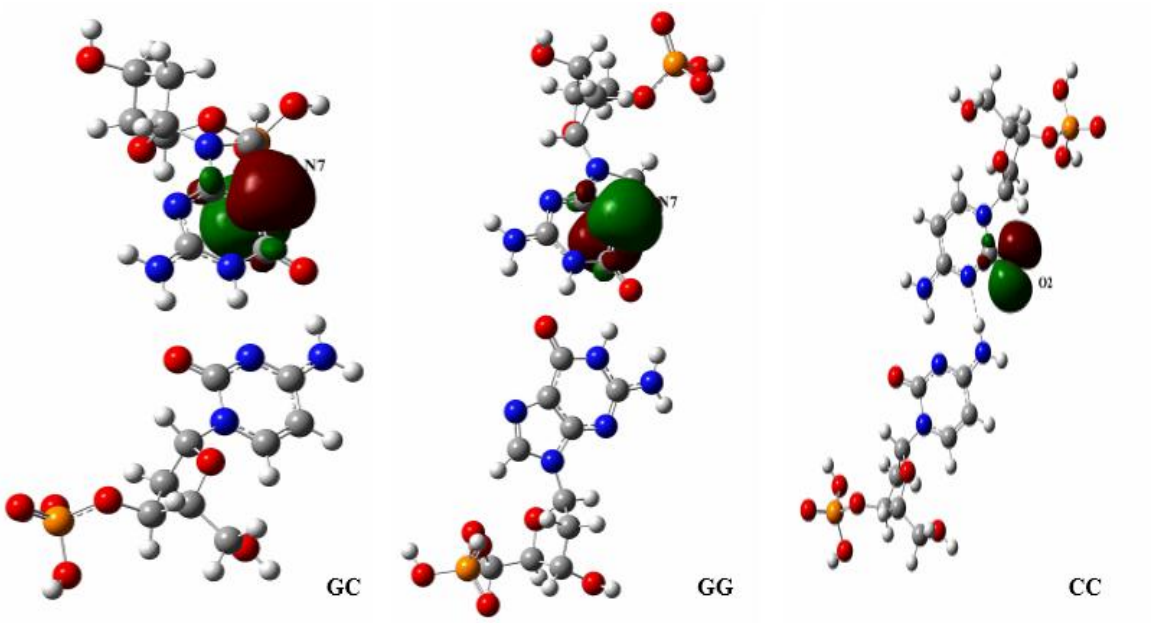

Fig. 6.5 Frontier HOMO diagrams of normal (**GC** and **AT**) and mismatch base pair (**GG**, **AA**, **TT** and **CC**).

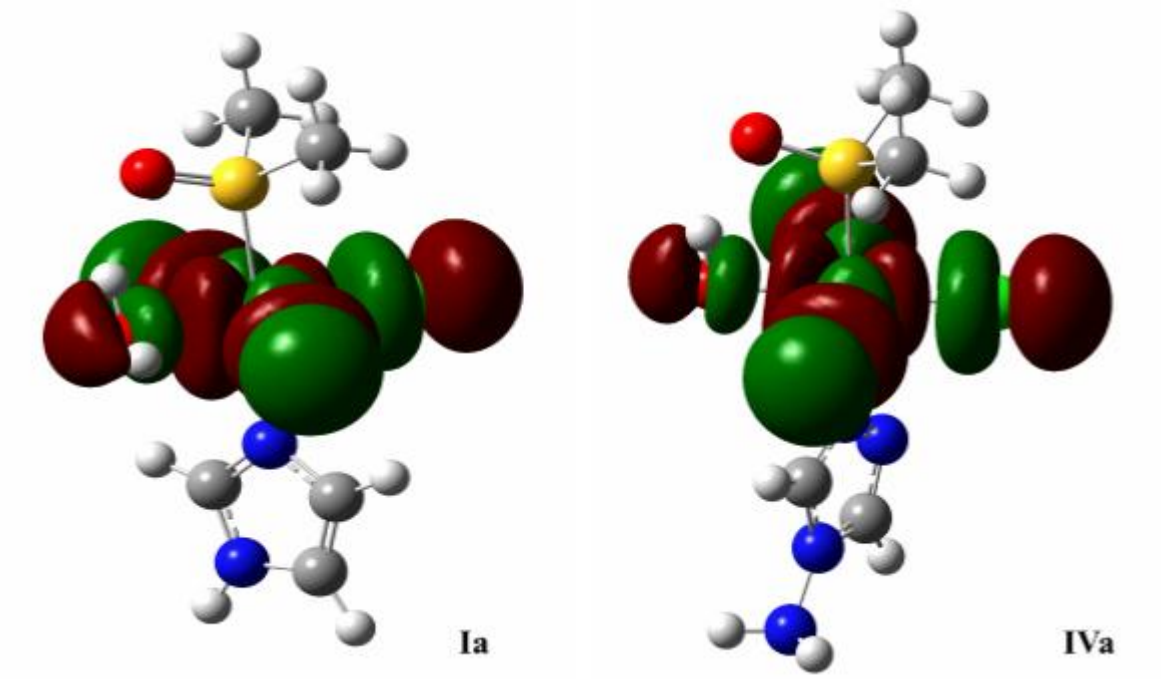

Fig. 6.6 Frontier LUMO diagrams of complex **Ia** and **IVa.**

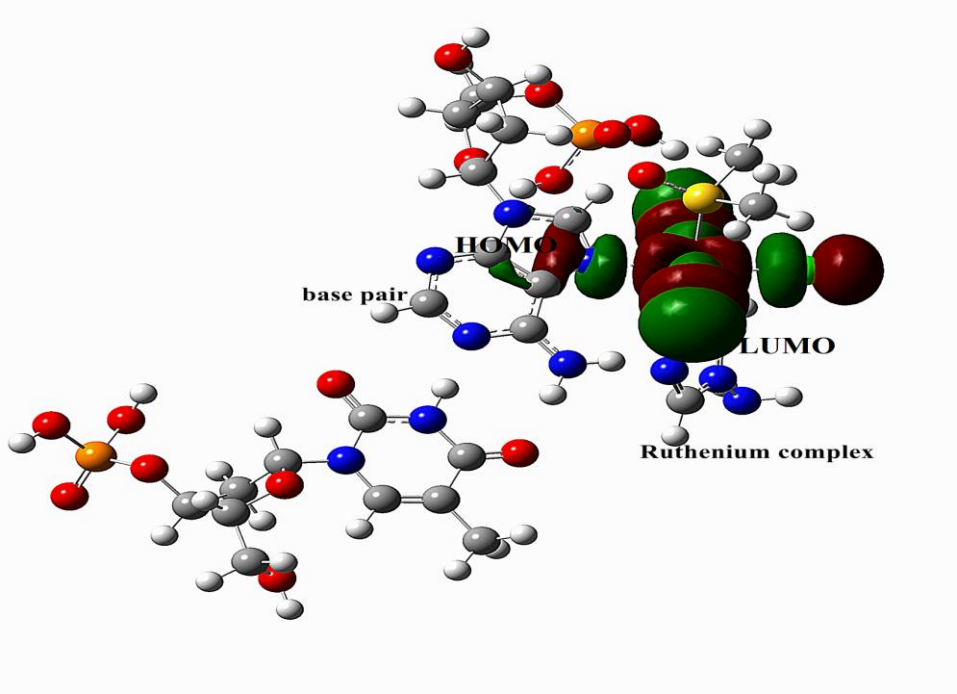

Fig.6.7 Base pair-ruthenium complex adduct (HOMO of base pair and LUMO of ruthenium complex).

6.3.4 Stability of ruthenium complex-base pair adduct

Stability of ruthenium complex-base pair adducts is investigated by evaluating the interaction energies at DFT- M062X level which are presented in Table 6.4 along with their absolute energy values. It is seen from Table 6.4 that interaction energy (ΔE) of **GC-Ia (**-15.060 kcal mol^{-1}) and **GC-IVa** (-16.943 kcal mol^{-1}) adducts are found to be lower than **AT-Ia (**-13.805 kcal mol^{-1}) and **AT-IVa (**-13.805 kcal mol^{-1}) adducts. Thus adducts of **GC** with complexes **Ia** and **IVa** are found to be more stable than **AT** adducts. The larger stability of the adduct with **GC** may be due to the presence of three hydrogen bonding in contrast to **AT** adducts where it has only two hydrogen bond. Ruthenium complex-mismatch base pair adducts, **GG-Ia** and **GG-IVa** have exhibited lowest interaction energy values of -19.452 and -18.198 kcal mol^{-1}, respectively than the **AA**, **CC** and **TT** adducts. Thus, calculated interaction energies suggest that **GC** and **GG** base pairs form stable adducts with ruthenium complexes than the other base pairs. Further **GG-Ia** and **GG-IVa** adducts exhibit higher absolute free energy values (Table 6.4) than other adducts. These results indicate that both the complexes show higher affinity toward mismatch **GG** base pair, in agreement with experimental results reported by Pluim *et. al*. and Groessl *et. al*.[40,41] However,

absolute energy values evaluated for **IVa-base pair** adducts are larger than that for **Ia-base pair** adducts. This may be due to the presence of primary amine group which favor the formation of strong hydrogen bonding, in agreement with experimental result.[42] Thus the observation reveals that complexes **Ia** and **IVa** interact well with the normal as well as mismatch base pairs of DNA.

Since all biological interactions are occur in aqueous environments, we have evaluated the interaction energy values for the ruthenium complex-base pair adducts in the aqueous medium. Solvent phase results evaluated at M062X / (LANL2DZ+6-31G (d,p)) level are summarized in Table 6.4. Interestingly, the solvent phase reactivity order of all the adducts are found to be different in comparison to their respective counterparts in the gas phase. This difference in reactivity trend may be due to the different extent of solvation for different adducts. On the other hand, ΔE of all adducts are observed to be lower in aqueous medium than their gas phase values, indicating decreased stability of all the adducts in aqueous medium. Thus in aqueous medium ruthenium complexes tend to interact with DNA base pairs more effectively.

Table 6.4 Absolute free energy values ($E_{rutehniumcomplex-basepair}$ in kcal mol^{-1}) of interacting adducts and calculated interaction energies (ΔE in kcal mol^{-1}) calculated at M062X /(LANL2DZ+6-31G(d,p)) level of theory.

Adduct	$E_{rutehniumcomplex-basepair}$ (gas phase)	$E_{rutehniumcomplex-basepair}$ (solvent phase)	ΔE (gas phase)	ΔE (solvent phase)
GC-Ia	830.823	826.430	-15.060	-11.295
GC-IVa	834.588	830.823	-16.943	-13.805
GG-Ia	853.413	849.020	-19.452	-7.530
GG-IVa	865.963	850.903	-18.198	-12.550
CC-Ia	808.232	805.722	-12.550	-11.923
CC-IVa	814.507	809.487	-11.923	-15.060
AT-Ia	846.510	840.235	-13.805	-12.550
AT-IVa	852.158	849.648	-13.805	-10.040
AA-Ia	845.255	842.745	-14.433	-9.413
AA-IVa	853.413	850.903	-11.923	-8.158
TT-Ia	849.648	847.765	-10.668	-4.393
TT-IVa	855.923	853.413	-10.040	-5.648

Stability of the ruthenium complex-base pair adducts not only depend on the number of hydrogen bonding but also on the mutual orientation of molecular dipole moments.[43] Stability of the adducts as well as the binding efficiency of ruthenium complexes with base pairs can be interpreted well with the help of calculated dipole moment(μ) values. DFT evaluated dipole moment (μ) of complexes **Ia** and **IVa**, their base pair adducts and isolated base pairs is listed in Table 6.5. The dipole moment of a molecule is observed due to the non-uniform distribution of charges on the various atoms in a molecule. The dipole moment is used primarily to interpret the intermolecular interactions involving the van der Waals type dipole–dipole forces.[44] Table 6.5 shows that dipole moment value of **GC** base pair (μ =10.223D) is higher than **AT** base pair (μ =5.100D) indicating that **GC** base pairs can form bond with metal complexes more efficiently. Hence, higher stability of **GC–Ia** and **GC-IVa** adduct can be explained from the dipole moment value of **GC** base pair. Again, deformation of base pairs that occurs upon interaction of ruthenium complexes is connected with the increased dipole moment value.[45] The dipole moment of **GG-Ia** adduct is 6.626 D and **GG-IVa** is 10.631 D while isolated **GG** base pair is 0.216D. These results reveal that **GG** base pair suffer more deformation when interacted with ruthenium complexes as compared to other base pairs (Table 6.5). Furthermore, dipole moment of the complexes **Ia** and **IVa** are found to be 3.055 and 4.689D, respectively. The higher dipole moment value for complex **IVa** leads to better binding interaction with DNA than complex **Ia**. Overall results indicate that the ruthenium complexes **Ia** and **IVa** can properly interact with DNA base pairs, inhibit their replication and subsequently prevent the redundant cell growth responsible for cancer cells.

Table 6.5 Calculated dipole moment (μ in D) values of ruthenium complex-base pair adducts calculated at M062X /(LANL2DZ+6-31G (d,p)) level.

Adducts	**Ia**	**IVa**	Isolated base pair
	μ	μ	μ
GC	13.061	14.956	10.223
GG	6.626	10.631	0.216
CC	9.200	8.713	4.090
AT	9.100	4.810	5.100
AA	7.333	8.190	2.686
TT	10.802	2.350	1.742
complex	3.066	4.689	

6.3.5 Natural Bond orbital (NBO) analysis

To obtain further insight into the nature of drug-DNA adducts, we have evaluated natural atomic charges and electronic configuration of all the atoms of the base pairs, ruthenium complexes and adducts by NBO analysis and results are summarized in Table 6.6. The calculated natural atomic charge on ruthenium ion in all the adducts are found to be lower than that of its formal charge +3. Atomic charge redistribution on all the atoms of the adducts can be observed when the atomic charges in the isolated base pairs and ruthenium complex-base pair adducts are compared. Calculated natural atomic charge on ruthenium atoms in the normal base pair adducts **GC-Ia**, **GC-IVa**, **AT-Ia** and **AT-IVa** are found to be +0.427, +0.435, +0.434 and +0.447, respectively, revealing a charge transfer phenomenon from base pair to ruthenium atom. Such charge transfer leads to decrease in the negative charge on O6 in guanine and O4 in thymine while, decrease in the positive charge on H4 (cytosine) and H6 (adenine) atoms (Table 6). Decreased negative charge on O6 partially reduces the strength of O6$^{\cdots}$H4 bond thereby increases the length of O6$^{\cdots}$H4 bond in **GC-Ia** as well as in **GC-IVa** adducts. On the other hand, lengthening of H6$^{\cdots}$O4 bond is in accordance with the decrease negative charge on O4 atom in **AT-Ia** and **AT-IVa** adducts. Similar type of atomic charge redistribution is observed in all other ruthenium complex-base pair adducts. From the results of NBO analysis, we found the electronic configuration of Ru in **GC-Ia** adduct as [core]$5s^{0.14}4d^{3.04}5p^{0.37}5d^{0.02}$, which contains 17.99 core electrons, 3.55 valence electrons (5s, 4d and 5p atomic orbitals) and 0.02 Rydberg electrons (mainly on 5d orbital). This gives rise to 21.56 electrons matches well with the calculated natural atomic charge on ruthenium atom (+0.427) in the adduct **GC-Ia**. Similar electronic configuration of ruthenium atom in all other adducts is noticed.

Table 6.6 Natural atomic charges and natural electron configuration of the selected atoms ruthenium complex-base pair adducts and isolated base pairs calculated at M062X /(LANL2DZ+6-31G (d,p)) level.

Adducts	Atoms	Base pair-**Ia**		Base pair-**IVa**		Isolated base pair	
		charge	electron configuration	charge	electron configuration	charge	electron configuration
GC	Ru	0.427	[core]$5s^{0.14}4d^{3.04}5p^{0.37}5d^{0.02}$	0.435	[core]$5s^{0.14}4d^{3.03}5p^{0.37}5d^{0.02}$		
	N7	-0.218	[core]$2s^{0.64}2p^{2.07}3p^{0.01}$	-0.213	[core]$2s^{0.59}2p^{2.12}$	-0.258	[core]$2s^{0.70}2p^{2.05}3d^{0.01}$
	O6	-0.339	[core]$2s^{0.84}2p^{2.49}3d^{0.01}$	-0.338	[core]$2s^{0.84}2p^{2.49}3d^{0.01}$	-0.342	[core]$2s^{0.84}2p^{2.49}3d^{0.01}$
	H4	0.235	$1s^{0.26}$	0.235	$1s^{0.26}$	0.236	$1s^{0.26}$
GG	Ru	0.434	[core]$5s^{0.14}4d^{3.03}5p^{0.37}5d^{0.02}$	0.439	[core]$5s^{0.14}4d^{3.03}5p^{0.37}5d^{0.02}$		
	N7	-0.229	[core]$2s^{0.64}2p^{2.08}3p^{0.01}$	-0.221	[core]$2s^{0.64}2p^{2.07}3p^{0.01}$	-0.231	[core]$2s^{0.70}2p^{2.02}3d^{0.01}$
	O6	-0.345	[core]$2s^{0.84}2p^{2.49}3d^{0.01}$	-0.352	[core]$2s^{0.84}2p^{2.50}3d^{0.01}$	-0.355	[core]$2s^{0.84}2p^{2.50}3d^{0.01}$
	H1	0.235	$1s^{0.26}$	0.235	$1s^{0.26}$	0.235	$1s^{0.26}$
CC	Ru	0.486	[core]$5s^{0.14}4d^{2.99}5p^{0.36}5d^{0.02}$	0.352	[core]$5s^{0.15}4d^{3.13}5p^{0.35}5d^{0.02}$		
	O2	-0.310	[core]$2s^{0.81}2p^{2.49}$	-0.271	[core]$2s^{0.80}2p^{2.46}$	-0.339	[core]$2s^{0.85}2p^{2.48}3d^{0.01}$
	N3	-0.340	[core]$2s^{0.68}2p^{2.15}3d^{0.01}$	-0.345	[core]$2s^{0.67}2p^{2.16}3p^{0.0}$	-0.343	[core]$2s^{0.68}2p^{2.15}3p^{0.01}3d^{0.01}$
	H4	0.232	$1s^{0.27}$	0.237	$1s^{0.26}$	0.237	$1s^{0.26}$
AT	Ru	0.434	[core]$5s^{0.14}4d^{3.03}5p^{0.38}5d^{0.02}$	0.447	[core]$5s^{0.14}4d^{3.01}5p^{0.37}5d^{0.02}$		
	N7	-0.231	[core]$2s^{0.64}2p^{2.08}3p^{0.01}$	-0.236	[core]$2s^{0.64}2p^{2.08}3p^{0.01}$	-0.245	[core]$2s^{0.70}2p^{2.04}3d^{0.01}$
	H6	0.222	$1s^{0.54}$	0.228	$1s^{0.27}$	0.244	$1s^{0.25}$
	O4	-0.327	[core]$2s^{1.69}2p^{4.96}3d^{0.01}$	-0.325	[core]$2s^{0.84}2p^{2.49}3d^{0.01}$	-0.335	[core]$2s^{0.68}2p^{2.13}3p^{0.01}$
AA	Ru	0.422	[core]$5s^{0.14}4d^{3.03}5p^{0.38}5d^{0.02}$	0.456	[core]$5s^{0.14}4d^{3.01}5p^{0.25}5d^{0.02}6p^{0.12}$		
	N7	-0.231	[core]$2s^{0.64}2p^{2.08}3p^{0.01}$	-0.230	[core]$2s^{0.64}2p^{2.08}3p^{0.01}$	-0.246	[core]$2s^{0.70}2p^{2.04}3d^{0.01}$
	N1	-0.310	[core]$2s^{0.68}2p^{2.12}3p^{0.01}3d^{0.01}$	-0.306	[core]$2s^{0.68}2p^{2.12}3p^{0.01}3d^{0.01}$	-0.314	[core]$2s^{0.68}2p^{2.12}3p^{0.01}3d^{0.01}$
	H6	0.229	$1s^{0.27}$	0.227	$1s^{0.27}$	0.232	$1s^{0.27}$
TT	Ru	0.431	[core]$5s^{0.14}4d^{3.03}5p^{0.37}5d^{0.02}$	0.447	[core]$5s^{0.14}4d^{3.02}5p^{0.37}5d^{0.02}$		
	O4	-0.296	[core]$2s^{0.81}2p^{2.48}$	-0.279	[core]$2s^{0.80}2p^{2.47}$	-0.303	[core]$2s^{0.85}2p^{2.45}3d^{0.01}$
	O2	-0.299	[core]$2s^{0.84}2p^{2.49}3d^{0.01}$	-0.298	[core]$2s^{0.84}2p^{2.49}3d^{0.01}$	-0.332	[core]$2s^{0.84}2p^{2.48}3d^{0.01}$
	H3	0.240	$1s^{0.25}$	0.239	$1s^{0.25}$	0.246	$1s^{0.25}$
complex	Ru	0.413	[core]$5s^{0.14}4d^{3.05}5p^{0.37}5d^{0.02}$	0.406	[core]$5s^{0.14}4d^{3.06}5p^{0.37}5d^{0.02}$		

6.4 Conclusion

Systematic DFT calculations have been carried out in order to analyze the geometry of normal, mismatch base pairs and their adducts with ruthenium complexes **Ia** and **IVa** at M062X/(LANL2DZ+6-31G(d, p)) level. Optimized geometries of the normal and mismatch base pairs are found to be nearly planar. However, upon interaction with ruthenium complex, the geometry of base pairs deviates from planarity. Both the complexes coordinated strongly with the imine sites of nucleobases through ruthenium atom, altering the geometry of base pairs. Among the normal base pairs, **GC** has shown higher interaction energy with ruthenium complexes than **AT** whereas **GG** mismatch base pair has the highest interaction energy followed by **AA**, **TT** and **CC**. Evaluated interaction energy suggests the higher stability of **GG** and **GC** adducts. Stability of all the adducts found to increase on inclusion of solvent effect. Further, higher absolute energy of **base pair-IVa** adducts than **base pair-Ia** adducts reveal higher reactivity of complex **IV** towards base pair, in agreement with experimental data. NBO analysis reveals that interaction in all the ruthenium complex-base pair adducts are mainly electrostatic in nature and charge transfer occurs from base pair to ruthenium complexes.

References

1. X. Tian, Y. Song, H. Dong, B. Ye, *Bioelectrochem*, 2008, **73**, 18–22.
2. M .Zewail-Foote, L. H. Hurley, *Anticancer Drugs Des*., 1999, **14**, 1–9.
3. S.F. Braga, L.C. de Melo, P. M. V. B. Barone, *J. Mol. Struct: Theochem*., 2004, **710**, 51–59.
4. T. Nishimura, T. Okobira, A. M. Kelly, N. Shimada, Y. Takeda, K. Sakurai, *BioChem*., 2007, **46**, 8156-8163.
5. M. Hossain, P. Giri, G .S. Kumar, *DNA Cell Biol*., 2008, **27**, 81–90.
6. P. Giri, G . S. Kumar, *Curr*. *Med*. *Chem*., 2009, **16**, 965–987.
7. S. Das, S. Kundu, G. S. Kumar, *DNA Cell Biol*., 2011, **30**, 525–535.
8. F. Lankas, T. E. Cheatham, N. Spackova, P. Hobza, J. Langowski, J. Sponer, *Biophys*., 2002, **82**, 2592–2609.
9. M.C. Hutter, *Chem. Phys*., 2006, **326**, 240–245.
10. T. A. Kunkel, *J. Biol. Chem*., 2004, **279**, 16895–16898.
11. W. Wang, H. W. Hellinga, L. S. Beese, *Proc. Natl. Acad. Sci. U. S. A*., 2011, **108**, 17644–17648.
12. M. Lichten, C. Goyon, N. P. Schultes, D. Treco, J. W. Szostak, J. E. Haber, A. Nicolas, *Proc. Natl. Acad. Sci. U. S. A*., 1990, **87**, 7653–7657.
13. K. S. Gates, *Chem. Res. Toxicol*., 2009, **22**, 1747–1760.
14. R. D. Bont, N. van Larebeke, *Mutagenesis*, 2004, **19**, 169–185.
15. E. C. Friedberg, *Nature*, 2003, **421**, 436–440.
16. P. Pourquier, J. Robert, *Bull. Cancer*, 2011, **98**, 229–237.
17. Z. Nagy, E. Soutoglou, *Trends Cell Biol*., 2009, **19**, 617–629.
18. J. H. J. Hoeijmakers, *Nature*, 2001, **411**, 366–374.
19. V. S. Li, D. Choi, Z. Wang, L. S. Jimenez, M. S. Tang, H. Kohn, *J. Am. Chem. Soc*., 1996, **118**, 2326–2331.
20. M. Tomasz, R. Lipman, D. Chowdary, J. Pawlak, G. L. Verdine, K. Nakanishi, *Science*., 1987, **235**, 1204–1208.
21. S. M. Hecht, *J. Nat. Prod*, 2000, **63**, 158–168.
22. G. Zuber, J. C. Quada, S. M. Hecht, *J. Am. Chem. Soc*., 1998, **120**, 9368–9369.
23. D. Frasca, J. Ciampa, J. Emerson, R. S. Umans, M. J. Clarke, *Metal Based Drugs.*, 1996, **3**, 197–201.

24. O. Novakava, J. Kaparova, O. Vrana, P. M. Van Vliet, J. Reedijk, V. Bravec, *Biochem.*,1995, **34**, 12369-12378.

25. A. Barca, B. Pani, M. Tamaro, E. Russo, *Mutat. Res*., 1999, **423**, 171-181.

26. E. Gallori, C. Vettori, E. Alessio, F. G. Vilchez, R. Vilaplana, P. Orioli, A. Casini, L. Messori, *Arch. Biochem. Biophy*., 2000, **376**, 156-162.

27. H. Hohmann, B. Hellquist, R. Van Eldik, *Inorg. Chem.*, 1992, **31**, 1090-1095.

28. M. J. Frisch, G. W. Trucks, H. B. Schlegel, G. E. Scuseria, M. A. Robb, J. R. Cheeseman, G. Scalmani, V. Barone, B. Mennucci, G. A. Petersson, H. Nakatsuji, M. Caricato, X. Li, H. P. Hratchian, A. F. Izmaylov, J. Bloino, G. Zheng, J. L. Sonnenberg, M. Hada, M. Ehara, K. Toyota, R. Fukuda, J. Hasegawa, M. Ishida, T. Nakajima, Y. Honda, O. Kitao, H. Nakai, T. Vreven, J .A. Montgomery, J. E. Peralta, F .Ogliaro, M. Bearpark, J. J. Heyd, E. Brothers, K. N. Kudin, V. N. Staroverov, T. Keith, R. Kobayashi, J. Normand, K. Raghavachari, A. Rendell, J. C. Burant, S. S. Iyengar, J .Tomasi, M. Cossi, N. Rega, J. M. Millam, M. Klene, J.E. Knox, J. B. Cross, V. Bakken, C. Adamo, J. Jaramillo, R. Gomperts, R. E. Stratmann, O. Yazyev, A. J. Austin, R.Cammi, C. Pomelli, J. W. Ochterski, R. L. Martin, K. Morokuma, V. G. Zakrzewski, G. A. Voth, P. Salvador, J. J. Dannenberg, S. Dapprich, A. D. Daniels, O. Farkas, J. B. Foresman, J. V. Ortiz, J. Cioslowski, D. J. Fox, Gaussian 09 Revision B.01.; *Gaussian Inc*.: Wallingford, CT, 2010.

29. Y. Zhao, D. G. Truhlar, *Theo. Chem. Acc*., 2008, **120**, 215–241.

30. P. J. Hay, W. R. Wadt, *J. Chem. Phys*., 1985, **82**, 270-284.

31. P. C. Hariharan, J. A. Pople, *Chem. Phys. Lett*., 1972, **16**, 217-219.

32. J. N. Harvey, *Annu. Rep. Prog. Chem., Sect*. C.: *Phys. Chem*., 2006, **102**, 203-226.

33. S. F. Boys, F. Bernardi, *Mol. Phys*., 1970, **19**, 553-566.

34. S. Simon, M. Duran, J. J. Dannenberg, *J. Chem. Phys*., 1996, **105**, 11024-11031.

35. E. Alessio, G. Balducci, A. Lutman, G. Mestroni, M. Calligaris, W. M. Attia, *Inorg. Chim. Acta*.,1993, **203**, 205-217.

36. J. Chen, L. Chen, S. Liao, K. Zheng, L. Ji, *J. Phys. Chem. B*, 2007, **111**, 7862-7869.

37. P .Deepa, P. Kolandaivel, K .S. Kumar, *Biophy Chem*., 2008, **136**, 50–58.

38. P. Deepa, P .Kolandaivel, K .S. Kumar, *Int J Quantum Chem*., 2011, **111**, 3239–3250.

39. K. Fukui, T. Yonezawa, H. Shingu, *J Chem. Phys*., 1952, **20**, 722–725.

40. D. Pluim, R. C. A. M. van Waardenburg, J. H. Beijnen, J. H. M. Schellens, *Cancer Chemother Pharm*., 2004, **54**, 71-78.

41. M. Groessl, Y. O. Tsybin, C. G. Hartinger, B. K. Keppler, P. J. Dyson, *J. Biol. Inorg. Chem*., 2010, **15**, 677–688.

42. M. Grossl, E. Reisner, C. G. Hartinger, R. Eichinger, O. Semenova, A. R. Timerbaev, M. A. Jakupec, V. B .Arion, B. K. Keppler, *J. Med. Chem*., 2007, **50**, 2185-2193.

43. P. Hobza, J. Sponer, *Chem. Rev*., 1999, **99**, 3247–3276.

44. H. A. R. Pramanik, D. Das, P. C. Paul, P. Mondal, C. R. Bhattacharjee, *J. Mol. Struc*., 2014, **1059**, 309–319.

45. J. V. Burda, J. Sponer, J. Leszczynski, P .Hobza, *J. Phys. Chem*., 1997, **101**, 9679-9677.